Science Bulletin 64 (2019) 1490–1495

Contents lists available at ScienceDirect

Science Bulletin

journal homepage: www.elsevier.com/locate/scib

Science Bulletin
www.scibull.com

Article

Flat-band ferromagnetism of SU(N) Hubbard model on Tasaki lattices

Ruijin Liu [a], Wenxing Nie [b,*], Wei Zhang [a,c,*]

[a] Department of Physics, Renmin University of China, Beijing 100872, China
[b] Center for Theoretical Physics, College of Physics, Sichuan University, Chengdu 610064, China
[c] Beijing Key Laboratory of Opto-electronic Functional Materials and Micro-nano Devices, Renmin University of China, Beijing 100872, China

ARTICLE INFO

Article history:
Received 11 May 2019
Received in revised form 14 July 2019
Accepted 1 August 2019
Available online 14 August 2019

Keywords:
SU(N)
Flat-band ferromagnetism
Percolation
Para-ferro transition

ABSTRACT

We investigate the para-ferro magnetic transition of the repulsive SU(N) Hubbard model on a type of one- and two-dimensional decorated cubic lattices, referred as Tasaki lattices, which feature massive single-particle ground state degeneracy. Under certain restrictions for constructing localized many-particle ground states of flat-band ferromagnetism, the quantum model of strongly correlated electrons is mapped to a classical statistical geometric site-percolation problem, where the nontrivial weights of different configurations must be considered. We prove rigorously the existence of para-ferro transition for the SU(N) Hubbard model on one-dimensional Tasaki lattice and determine the critical density by the transfer-matrix method. In two dimensions, we numerically investigate the phase transition of SU(3), SU(4) and SU(10) Hubbard models by Metropolis Monte Carlo simulation. We find that the critical density exceeds that of standard percolation, and increases with spin degrees of freedom, implying that the effective repulsive interaction becomes stronger for larger N. We further rigorously prove the existence of flat-band ferromagnetism of the SU(N) Hubbard model when the number of particles equals to the degeneracy of the lowest band in the single-particle energy spectrum.

1. Introduction

In condensed matter physics, the interplay of the Coulomb interaction with Pauli principle is a fundamental problem, from where many intriguing phases can appear. One important problem is the emergence of ferromagnetism in two or higher dimensions, which can date back to the early age of quantum theory and reveal the importance of many-body effect. After more than one century of investigation, a few special cases have been solved by either exact results [1–9] or sign-problem-free quantum Monte Carlo simulation [10]. However, a general solution to this problem is still lack, partly due to the notorious sign problem of fermions [11,12]. As an interesting and important limiting case, a system with a flat band in the single-electron energy spectrum may favor the stabilization of ferromagnetism as it reduces the kinetic energy cost for spin polarization to zero due to the band flatness. For instance, Mielke and Tasaki [3–6] proved flat-band ferromagnetism in a class of lattices, based on a systematic route called "cell construction". After that, flat-band ferromagnetism has attracted a lot of attention and has been connected with the discussion of topological and magnetic phases [13–21].

The previous investigation on flat-band ferromagnetism mainly focused on fermionic systems possessing the SU(2) spin-rotational symmetry. The SU($N > 2$) generalization of flat-band ferromagnetism is not only of theoretical interests [22–30], but also of experimental relevance in the context of cold atomic gases [31–34], where the high degrees of freedom of nuclear spin provide a fascinating playground to simulate the SU(N) fermionic Hubbard model [35–38]. By loading ultracold alkaline-earth-metal(-like) atoms in different optical lattices, the quantum simulation of various models has been theoretically proposed and further experimentally realized [31,32,39,40], where the spin symmetries can be as high as SU(6) for ^{173}Yb [32,33,41,42] and SU(10) for ^{87}Sr [39,43].

In this paper, we investigate the para-ferro magnetic transition and flat-band ferromagnetism of the SU(N) Hubbard model on a special class of decorated cubic lattices in one and two dimensions, which are illustrated in Fig. 1. The existence of ferromagnetism with SU(2) spin symmetry on this lattice, later referred as Tasaki lattice for short, is first considered by Mielke and Tasaki [3–6], and further by Maksymenko et al. [44], who introduced a mapping from the quantum Hubbard model to a classical statistical geometric site-percolation problem. Here, we first prove a generalized version of this mapping from the SU(N) Hubbard model to an N-state Pauli-correlated percolation (PCP) problem, where an SU(N)

* Corresponding authors.
E-mail addresses: wenxing.nie@gmail.com (W. Nie), wzhangl@ruc.edu.cn (W. Zhang).

https://doi.org/10.1016/j.scib.2019.08.013
2095-9273/

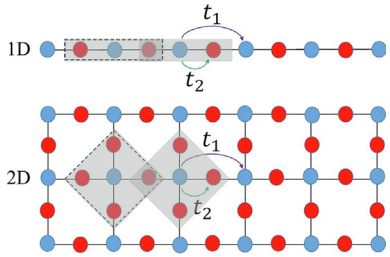

Fig. 1. (Color online) An illustration of the decorated cubic lattices designed by Tasaki in 1D and 2D: blue sites denote the undecorated hypercubic lattice, and the red ones denote the decorated sites. A trapping cell indicated by dashed-line area contains three (five) sites for 1D (2D) Tasaki lattice. The shaded area in grey shows an example of cluster of length two, with the overlapping of two adjacent trapping cells.

correlated weight for each configuration is considered. Then we obtain the exact results in one-dimensional (1D) Tasaki lattice for the SU(N) Hubbard model, and further verify the para-ferro magnetic transition numerically. For the two-dimensional (2D) case, we implement importance samplings by Metropolis Monte Carlo simulation and determine the para-ferro magnetic transition numerically. Moreover, we prove rigorously the existence of flat-band ferromagnetism of the SU(N) Hubbard model, when the number of particles n equals to the degeneracy $\mathcal{N}$ of the lowest band in the single-particle energy spectrum.

2. Mapping from the SU(N) Hubbard model to an N-state Pauli-correlated percolation problem

We start with the SU(N) Hubbard model with repulsive interaction $U > 0$ on a Tasaki lattice Λ,

$$H = \sum_{ij\in\Lambda} t_{ij}\left(c^{\dagger}_{i,\sigma}c_{j,\sigma} + \text{H.c.}\right) + U\sum_{i}\sum_{\sigma\neq\sigma'} n_{i,\sigma}n_{i,\sigma'}, \tag{1}$$

where $\sigma = \{1,\cdots,N\}$ labels the spin (or equivalently flavor or color) of a fermion. The operator $c_{i,\sigma}$ and its adjoint $c^{\dagger}_{i,\sigma}$ satisfy the fermionic anticommutation relations $\{c^{\dagger}_{i,\sigma}, c_{j,\sigma'}\} = \delta_{ij}\delta_{\sigma\sigma'}$ and $\{c_{i,\sigma}, c_{j,\sigma}\} = \{c^{\dagger}_{i,\sigma}, c^{\dagger}_{j,\sigma}\} = 0$, and the number operator $n_{i,\sigma} \equiv c^{\dagger}_{i,\sigma}c_{i,\sigma}$. The Tasaki lattice Λ is a d-dimensional hypercubic lattice with decorated sites located at the middle of the nearest links of the hypercubic lattice [7]. The hopping pattern, therefore, is composed by the nearest-neighbor ones (t_1) on the original hypercubic lattice and the nearest-neighbor ones (t_2) after the decoration, as shown in Fig. 1.

The lowest band of single-particle energy spectrum of the Tasaki lattice is completely dispersionless as long as $t_2 = \sqrt{c}\,t_1 > 0$, in which c is the coordination number of the corresponding undecorated lattice ($c = 2$ and $c = 4$ for 1D and 2D lattices, respectively). The existence of flat band is due to destructive interferences of particle hoppings, implying that we can construct the localized single-particle eigenstate in each trapping cell [45–48], whose wave function only overlaps with that of particles in adjacent cells, as shown by dark grey areas in Fig. 1. When non-interacting particles are filled into the flat band, the ground states are highly degenerate respective to the spin of individual particles. The ferromagnetic state with all particles possess the same spin is obviously one of these degenerate ground states.

Since the repulsive interaction is positive semidefinite, the ground state energy may not decrease as one turns on $U > 0$. In the limit of low particle density, each trapping cell is occupied by at most one particle to avoid energy penalty. When the density increases, the wave function of a trapping cell can not avoid overlapping with that of adjacent one. But the energy penalty can be avoided as well if the particles in neighboring trapping cells are in the same symmetric spin state [44]. By doing so, particles on these linked trapping cells are aligned in spin, and form a polarized "cluster" as shown in Fig. 2a. Namely, the minimization of energy requires all spins of particles belonging to the same cluster to be aligned, and this is the origin of ferromagnetism.

We then establish a one-to-one correspondence between the states composed of ferromagnetic clusters and the geometric configurations of n ($\leqslant \mathcal{N}$) particles distributed over $\mathcal{N}$ traps. In comparison to the standard percolation [49,50], the ferromagnetic state of a cluster C of size $|C|$ (or the number of particles in cluster C) acquires an additional spin degeneracy, which is given by the dimension of the irreducible representation of the SU(N) group [51,52],

$$d_{\text{SU}(N)}(|C|) = (N + |C| - 1)!/(|C|!(N-1)!). \tag{2}$$

For example, the degeneracy of the ferromagnetic state in the SU(2) Hubbard model is $2S + 1$, where S is the total spin of this cluster. Therefore, for a ferromagnetic cluster of length three and with total spin $S = 3/2$ as shown on the left side of Fig. 2a, we need to assign a factor of 4 to the geometric configuration of the cluster composed by three linked trapping cells depicted on the left of Fig. 2b. Note that the irreducible representation is the "permutation symmetric" representation of the SU(N) group. As the ferromagnetic cluster carries the fully symmetric representation of the SU(N) group, the electron wave function is fully antisymmetric in the spatial space, thereby avoiding the interaction energy penalty. Thus, for a given configuration q composed by a set of linked clusters, a nontrivial weight $W(q)$ must be assigned by taking into account the spin degeneracy of each cluster

$$W(q) = \prod_{i=1}^{M_q} \mathrm{e}^{\mu|C_i|} d_{\text{SU}(N)}(|C_i|), \tag{3}$$

where e^{μ} is the fugacity to tune the number of particles in a grand-canonical ensemble. Further analysis shows that for a given number of particles, the relative probability for them to decompose into smaller clusters is higher than forming larger clusters, which implies that this nontrivial weight gives rise to an effective repulsive interaction, tending to break up large clusters [44]. In the following model calculation, it will be shown that the repulsive effect becomes stronger with N, such that the formation of clusters with size proportional to the system size, i.e., the percolation transition, becomes more difficult in systems with higher SU(N) spin symmetry.

The key theorem then needs to be proved is that the ground states of the SU(N) Hubbard model when the flat band is partially filled can be represented by the states of ferromagnetic clusters, which can further be mapped into geometric configurations (see the Supplementary material). Then the quantum many-body system of SU(N) flat-band ferromagnetism is reduced to a classical site-percolation problem with a nontrivial weight. The expectation value of an operator O is the average over all degenerate ground states,

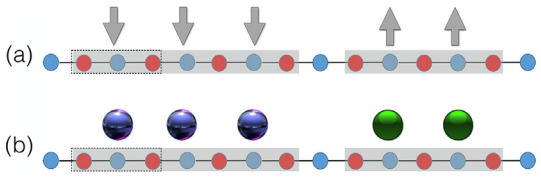

Fig. 2. (Color online) An illustration of the mapping between (a) the ferromagnetic states and (b) the configuration of linked clusters of percolation of 2-color particles. The shaded areas in grey show examples of ferromagnetic clusters in (a) and linked occupied trapping cells in the perspective of percolation in (b). A trapping cell is illustrated by the area enclosed by the dashed-lines.

$$\langle O\rangle = \frac{\sum_q O_q W(q)}{\sum_q W(q)}. \tag{4}$$

For the sake of magnetism, we consider the total spin operator $\mathbf{S}$ and focus on the expectation value $\langle \mathbf{S}^2\rangle = \sum_q S_q^2 W(q)/\sum_q W(q)$, where $\mathbf{S}^2$ is the quadratic Casimir operator of the SU(N) group. Because the particles belonging to the same cluster are aligned in the ferromagnetic state, the eigenvalue of $\mathbf{S}^2$ for a cluster with size $|C|$ is [53]

$$S^2(|C|) = \frac{(N-1)(N+|C|)|C|}{2N}. \tag{5}$$

The total spin $\mathbf{S}_q^2$ for a given geometric configuration q can be calculated in two equivalent ways

$$\begin{aligned} S_q^2 &= \sum_{i=1}^{M_q} S^2(|C_i|) \\ &= \sum_{l=1}^{n} N_q(l) S^2(l) = \mathcal{N}\sum_{l=1}^{n} n_q(l) S^2(l), \end{aligned} \tag{6}$$

where $N_q(l)$ is the number of clusters of size l, and $n_q(l) \equiv N_q(l)/\mathcal{N}$ is the normalized fraction with respect to the number of traps $\mathcal{N}$. The average value of the fraction $n(l) = \sum_q n_q(l) W(q)/\sum_q W(q)$ is a characteristic quantity in percolation as it signals the information of cluster size distribution [49,50].

3. Exact results in one dimension

As we have discussed in the previous section, the many-body ground states of the SU(N) Hubbard model on flat bands can be mapped to a geometric site-percolation problem with a nontrivial weight. In this section, we consider the 1D Tasaki lattice as an example, and present some exact results obtained by the transfer-matrix method [44]. The most important step is to construct a one-to-one mapping between the enumeration of all ground states of the Hubbard model and the counting of configurations when populating n particles with spin component $1, 2, \cdots, N$ into $\mathcal{N}$ trapping cells. Here, we establish such a mapping by introducing the following rules to populate particles with spin component $\sigma = 1, 2, \cdots, N$ to the trapping cells [54]:

(1) Each trap j can be either empty or occupied by only one particle with spin component σ. In other words, for each trap $j = 0, 1, \cdots, \mathcal{N}-1$, there are $N+1$ trap states $\sigma_j = 0, 1, \cdots, N$, where 0 indicates the trap is empty. Then a ground state of the chain is presented as a sequence of the trap states.
(2) We take the convention $\sigma_i \leqslant \sigma_{i+1}$ to avoid over counting, because only one sequence of two trap states corresponding to the neighboring cells occupied by different spin-component particles is allowed when moving along adjacent traps.

After employing the two rules above, we can construct a transfer matrix $\mathbf{T}$ to represent the percolation problem, where the grand partition function is given by $\Xi(z, \mathcal{N}) = \mathrm{Tr}\mathbf{T}^{\mathcal{N}}$ (see the Supplementary material). Fig. 3 shows the cluster distribution $n(l)$ and the macroscopic magnetic moment $S^2/S^2_{\max}$ of the Hubbard model with SU(3), SU(4) and SU(10) symmetries for instances, at the particle density $p \equiv n/\mathcal{N} = 0.99$. For the cluster distribution $n(l)$ depicted in Fig. 3a, a non-monotonic behavior with a peak structure at some finite l and vanishing value for large enough cluster is observed for all cases. With increasing N, the peak becomes higher and narrower, with the central position shifted to a larger value of l. This

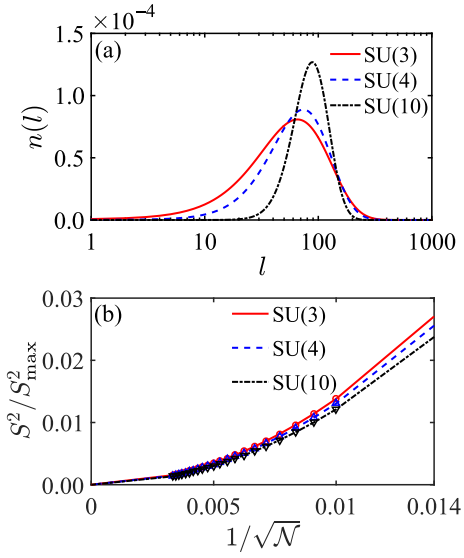

Fig. 3. (Color online) (a) Cluster distributions and (b) macroscopic magnetic moments in 1D Tasaki lattice for the Hubbard model with SU(3), SU(4) and SU(10) symmetries. The particle density $p = 0.99$ and the number of trapping cells $\mathcal{N} = 10^5$ are chosen for calculation in all cases. The macroscopic magnetic moments $S^2_{\max}$ is determined by arranging all particles within one single cluster.

tendency indicates that the effective repulsion induced by the nontrivial weight is more prominent for cases of higher spin symmetry. From Fig. 3b, we find that the macroscopic magnetic moment scales to zero for all cases, implying that the ground state is still paramagnetic when the flat band is nearly $1/N$ filled. Besides, the macroscopic magnetic moment for SU(10) is smaller than that of SU(3) at the same concentration. This observation suggests that the formation of large enough clusters is more difficult in SU(10) system than the SU(3) case, as can also be inferred from the tails on the right side of Fig. 3a. We will find these results consistent with following analytic discussions.

In the thermodynamic limit ($\mathcal{N} \to \infty$ with $n/\mathcal{N}$ finite), we obtain the cluster distribution

$$n(l, \mathrm{SU}(N)) = f_{\mathrm{SU}(N)}(z)\frac{(l+N-1)!}{l!}\left(\frac{z}{\lambda_{\max}(z)}\right)^l, \tag{7}$$

where $z = \mathrm{e}^{\mu}$ is the fugacity, $f_{\mathrm{SU}(N)}(z)$ is a function depends only on z and N, and $\lambda_{\max}(z)$ is the eigenvalue with maximal modulus of the $\mathbf{T}$-matrix. The exact expression of $f_{\mathrm{SU}(N)}(z)$ is in general complicated, but fortunately we can treat it as a coefficient function such that some important properties of the system, including the shape of the cluster distribution $n(l)$, can be obtained qualitatively. From Eq. (7), one can easily conclude that as long as $z/\lambda_{\max}(z) < 1$, clusters of large enough size must vanish. The percolation transition thus occurs when the condition $z_c/\lambda_{\max}(z_c) = 1$ is satisfied, which results in $z_c \to +\infty$ (see the Supplementary material).

For the macroscopic magnetic moment, we have

$$\frac{S^2}{\mathcal{N}^2} = \sum_{l=1}^{n}\frac{S_l^2}{\mathcal{N}} f_{\mathrm{SU}(N)}(z)\frac{(l+N-1)!}{l!}\left(\frac{z}{\lambda_{\max}}\right)^l, \tag{8}$$

which also proves the ground state is paramagnetic for finite z. Further calculation shows that in the thermodynamic limit, the particle density p indeed approaches unity as $z \to +\infty$. Hence the ground state is paramagnetic at any particle density $p < 1$ for arbitrary N, with an onset of ferromagnetism at $p = 1$. These results are consistent with our rigorous proof of flat band ferromagnetism for SU(N) Hubbard model on the Tasaki lattice at filling $p = 1$ (see the Supplementary material). One should remind that the conclusions stated above does not contradict with the Lieb-Mattis theorem [55], which proves the

absence of ferromagnetism of 1D Hubbard model on lattices without loops. However, here we consider a special type of lattices with loops composed by nearest t_1 and next-nearest neighbor hoppings t_2 as depicted in Fig. 1. In fact, as the existence of loop is crucial to validate the construction of the many-body ground states [7,56,57], the Lieb-Mattis theorem does not apply in this circumstance.

4. Para-ferro magnetic transition in two dimensions

For 2D Tasaki lattice, the transfer matrix formalism employed above can not be directly applied [58]. For instead, we make use of the Metropolis Monte Carlo method with importance samplings for the nontrivial weights to simulate the percolation problem on 2D $L \times L$ Tasaki lattices with periodic boundary conditions. A new configuration is accepted with the Metropolis probability $\min[1, W(q')/W(q)]$, in which q denotes the old configuration and q' denotes a new configuration. Specifically, to obtain the density of particles versus fugacity $z = e^{\mu}$, we perform grand-canonical simulations with exchange Monte Carlo. We randomly choose a site and change its occupying status, i.e., if it is (not) occupied, we (populate) remove one particle.

The percolation transition can be identified as a first order jump between concentrations p_- and p_+ shown in Fig. 4. For fillings below p_-, the possibility to find a cluster of the same color

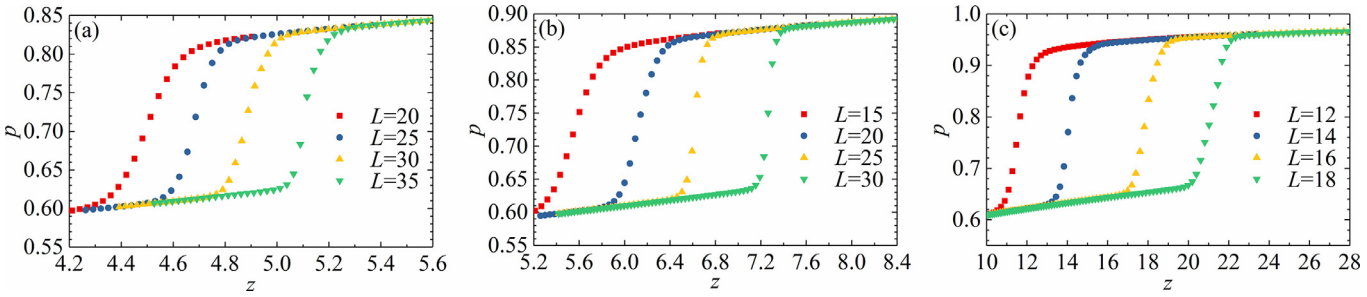

Fig. 4. (Color online) Particle density p versus fugacity z in 2D Tasaki lattice for the Hubbard model with (a) SU(3), (b) SU(4) and (c) SU(10) symmetries.

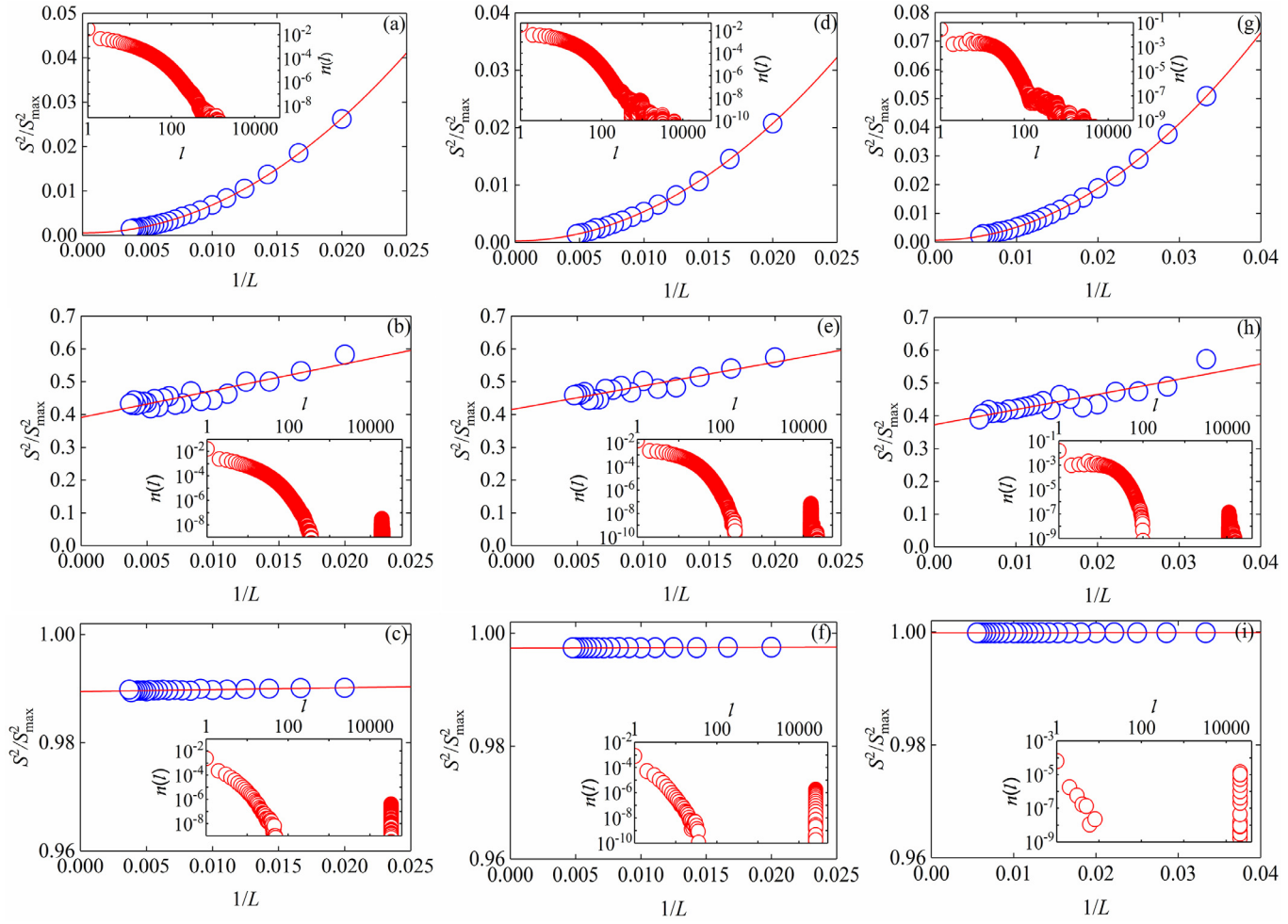

Fig. 5. (Color online) Macroscopic magnetic moment S^2/S^2_{max} for 2D Tasaki lattice. For the SU(3) case, numerical results (green circles) are depicted for system size up to $L = 270$ at particle densities (a) $p = 0.64$, (b) $p = 0.74$, (c) $p = 0.83$. For the SU(4) case, lattice size is up to $L = 210$ with particle densities (d) $p = 0.65$, (e) $p = 0.77$, (f) $p = 0.88$. For the SU(10) case, lattice size is up to $L = 200$ and the particle densities are chosen as (g) $p = 0.69$, (h) $p = 0.82$, (i) $p = 0.95$. The maximal magnetic moment S^2_{max} is calculated by arranging all particles in one single cluster. The insets show cluster distributions with $L = 200$ for SU(3), $L = 170$ for SU(4), and $L = 150$ for SU(10), respectively.

is vanishingly small in the thermodynamic limit, suggesting a paramagnetic state in the original Hubbard model. When $p > p_+$, the clusters of the same color can be linked together to reach a macroscopic size. In the SU(N) Hubbard model, this regime corresponds to a system with a macroscopic ferromagnetic domain.

In order to determine the para-ferro magnetic transition point, we perform canonical simulations with fixed density of particles for various lattice sizes L to obtain the macroscopic magnetic moments, and extrapolate the results to the thermodynamic limit. Numerically, we generate a new configuration q' from the old one q by randomly permuting the occupied status of two sites to guarantee the constraint that the number of particles is fixed. As shown in Fig. 5a, d and g, the macroscopic magnetic moments scale to zero at $p = 0.64$ for the SU(3) Hubbard model, at $p = 0.65$ for the SU(4) model, and at $p = 0.69$ for the SU(10) case. This implies that the corresponding ground states are paramagnetic below such fillings. In Fig. 5b, e and h, the particle densities are increased to $p = 0.74, 0.77$, and 0.82 for the SU(3), SU(4), and SU(10) models, respectively. The macroscopic magnetic moments in all cases scale to a finite values in the thermodynamic limit, indicating the emergence of ferromagnetism. In this regime, the snapshot (see the Supplementary material) shows the concomitant phase-separated states, where macroscopic ferromagnetic domains can be observed. In Fig. 5c, f and i, the particle density is further enhanced to $p = 0.83, 0.88$, and 0.95 for the SU(3), SU(4), and SU(10) cases, respectively. The macroscopic magnetic moments scale to finite values with $S^2/S^2_{\max} \approx 1$ in the thermodynamic limit, and are independent of the system size. In this regime, the snapshot shows the ferromagnetic phase spans across the entire system.

Based on the numerical results in both grand canonical and canonical ensembles, we obtain the phase diagrams for SU(N) Hubbard models on 2D Tasaki lattice. By increasing particle density p, the para-ferro transition as a first order jump is found to lay between concentrations $p_-$and p_+, whose exact values are both enhanced with N. When $p < p_-$, the ground state is paramagnetic with zero macroscopic magnetic moment. When $p_- < p < p_+$, the ground state falls into the phase-separation regime of ferromagnetic domains. As $p_+ < p < 1$, the ground state is of unsaturated ferromagnetism, where the ferromagnetic phase spans across the entire system. The dependence of the exact values of p_- and p_+ on the value of N is rooted from the stronger effective repulsion in systems with larger N. Finally, as the flat band is $1/N$ filled with $p = 1$, the ground state for arbitrary N is rigorously proved to be the ferromagnetic state (see the Supplementary material).

It is interesting to consider the limit $N \to \infty$, where a numerical calculation becomes difficult by directly using the method discussed above due to the largely extended space of spin degrees of freedom. This difficulty may be overcome by employing the very large symmetry of the system and mapping to other more tractable models. From our Monte Carlo simulation results and in the view that the effective repulsive interaction that leads to the breakup of the large clusters increases with larger N, the para-ferro transition is expected to occur only at $p = 1$ when N goes to infinity. The conjecture coincides with the rigorous proof that the ground state at $p = 1$ is of saturated flat-band ferromagnetism (see the Supplementary material). In this limit $N \to \infty$, the ground state is paramagnetic as long as $p < 1$ for both 1D and 2D cases.

5. Conclusions

We study the Hubbard models with SU(N) spin symmetry and repulsive interaction on a type of decorated cubic lattices in one and two dimensions, where flat bands are present at the bottom of the band structures. When the filling density $p \equiv n/\mathcal{N} \leq 1$ with n the number of particles and $\mathcal{N}$ the single particle flat band degeneracy, we prove that the ground states of the SU(N) Hubbard model can be mapped to the geometrical configuration of an N-state Pauli-correlated percolation problem with a nontrivial weight. Based on this exact mapping, we solve for the ground states for 1D Tasaki lattice by a transfer-matrix method, and conclude that the system is paramagnetic at density $p < 1$ for arbitrary N. For 2D cases, we consider the SU($N = 3, 4, 10$) symmetries as typical examples, and use the Metropolis Monte Carlo method to obtain the ground states numerically. The para-ferro magnetic transition point p_c is estimated to lay between $p_- < p_c < p_+$ with $p_-(N = 3) = 0.64(1)$, $p_+(N = 3) = 0.83(0)$, $p_-(N = 4) = 0.65(1)$, $p_+(N = 4) = 0.87(7)$, $p_-(N = 10) = 0.69(4)$, $p_+(N = 10) = 0.94(5)$. We also prove rigorously the existence of flat-band ferromagnetism for all values of $N \geqslant 2$ in arbitrary dimension, provided that the number of particles equals to the degeneracy of the flat band in the single-particle energy spectrum. The present problem reduces to the standard site percolation problem by taking $N = 1$.

Conflict of interest

The authors declare that they have no conflict of interest.

Acknowledgments

R.L. and W.Z. are supported by the National Key R&D Program of China (2018YFA0306501), the National Natural Science Foundation of China (11434011, 11522436, and 11774425), the Beijing Natural Science Foundation (Z180013), and the Research Funds of Renmin University of China (10XNL016 and 16XNLQ03). W.N. is supported in part by the National Key R&D Program of China (2017YFB0405700), the National Natural Science Foundation of China (11704267) and start-up funding from Sichuan University (2018SCU12063). We would like to thank Zheng-Xin Liu, Deping Zhang and Zi-Xiang Li for helpful discussions.

Author contributions

W. Nie and W. Zhang conceived the project. All authors contributed equally to the analytical calculation. R. Liu and W. Nie performed the Metropolis Monte Carlo simulation for the 2D case. W. Nie and W. Zhang wrote the manuscript with inputs from all coauthors.

Appendix A. Supplementary material

Supplementary material to this article can be found online at https://doi.org/10.1016/j.scib.2019.08.013.

References

[1] Nagaoka Y. Ferromagnetism in a narrow, almost half-filled s band. Phys Rev 1966;147:392–405.
[2] Lieb EH. Two theorems on the Hubbard model. Phys Rev Lett 1989;62:1201–4.
[3] Mielke A. Ferromagnetic ground states for the Hubbard model on line graphs. J Phys A: Math Gen 1991;24:L73.
[4] Mielke A. Ferromagnetism in the Hubbard model on line graphs and further considerations. J Phys A: Math Gen 1991;24:3311.
[5] Tasaki H. Ferromagnetism in the Hubbard models with degenerate single-electron ground states. Phys Rev Lett 1992;69:1608–11.
[6] Mielke A, Tasaki H. Ferromagnetism in the Hubbard model. Commun Math Phys 1993;158:341–71.
[7] Tasaki H. From Nagaoka's ferromagnetism to flat-band ferromagnetism and beyond: an introduction to ferromagnetism in the Hubbard model. Prog Theor Phys 1998;99:489–548.
[8] Li Y, Lieb EH, Wu CJ. Exact results for itinerant ferromagnetism in multiorbital systems on square and cubic lattices. Phys Rev Lett 2014;112:217201.

[9] Bobrow E, Stubis K, Li Y. Exact results on itinerant ferromagnetism and the 15-puzzle problem. Phys Rev B 2018;98:180101.
[10] Xu SL, Li Y, Wu CJ. Sign-problem-free quantum Monte Carlo study on thermodynamic properties and magnetic phase transitions in orbital-active itinerant ferromagnets. Phys Rev X 2015;5:021032.
[11] Lieb EH. Advances in dynamical systems and quantum physics. Singapore: World Scientific; 1995. p. 173–93.
[12] Essler FHL, Frahm H, Göhmann F, et al. The one-dimensional Hubbard model. Cambridge: Cambridge University Press; 2005.
[13] Sheng DN, Gu ZC, Sun K, et al. Fractional quantum Hall effect in the absence of Landau levels. Nat Commun 2011;2:389.
[14] Sun K, Gu ZC, Katsura H, et al. Nearly flatbands with nontrivial topology. Phys Rev Lett 2011;106:236803.
[15] Tang E, Mei JW, Wen XG. High-temperature fractional quantum Hall States. Phys Rev Lett 2011;106:236802.
[16] Katsura H, Maruyama I, Tanaka A, et al. Ferromagnetism in the Hubbard model with topological/non-topological flat bands. Europhys Lett 2010;91:57007.
[17] Scaffidi T, Simon SH. Exact solutions of fractional Chern insulators: interacting particles in the Hofstadter model at finite size. Phys Rev B 2014;90:115132.
[18] Essafi K, Jaubert LDC, Udagawa M. Flat bands and Dirac cones in breathing lattices. J Phys: Conden Matt 2017;29:315802.
[19] Tsai WF, Fang C, Yao H, et al. Interaction-driven topological and nematic phases on the Lieb lattice. New J Phys 2015;17:055016.
[20] Goldman N, Urban DF, Bercioux D. Topological phases for fermionic cold atoms on the Lieb lattice. Phys Rev A 2011;83:063601.
[21] Zhang SZ, Hung HH, Wu CJ. Proposed realization of itinerant ferromagnetism in optical lattices. Phys Rev A 2010;82:053618.
[22] Affleck I, Marston JB. Large-n limit of the Heisenberg-Hubbard model: implications for high-T_c superconductors. Phys Rev B 1988;37:3774–7.
[23] Marston JB, Affleck I. Large-n limit of the Hubbard-Heisenberg model. Phys Rev B 1989;39:11538–58.
[24] Read N, Sachdev S. Spin-Peierls, valence-bond solid, and Néel ground states of low-dimensional quantum antiferromagnets. Phys Rev B 1990;42:4568–89.
[25] Read N, Sachdev S. Valence-bond and spin-Peierls ground states of low-dimensional quantum antiferromagnets. Phys Rev Lett 1989;62:1694–7.
[26] Wu CJ, Hu JP, Zhang SC. Exact SO(5) symmetry in the spin-3/2 fermionic system. Phys Rev Lett 2003;91:186402.
[27] Wu CJ. Mott made easy. Nat Phys 2012;8:784–5.
[28] Wu CJ. Viewpoint: exotic many-body physics with large-spin Fermi gases. Physics 2010;3:92.
[29] Cazalilla MA, Ho AF, Ueda M. Ultracold gases of ytterbium: ferromagnetism and Mott states in an SU(6) Fermi system. New J Phys 2009;11:103033.
[30] Nie WX, Zhang DP, Zhang W. Ferromagnetic ground state of the SU(3) Hubbard model on the Lieb lattice. Phys Rev A 2017;96:053616.
[31] Fukuhara T, Takasu Y, Kumakura M, et al. Degenerate fermi gases of ytterbium. Phys Rev Lett 2007;98:030401.
[32] Taie S, Yamazaki R, Sugawa S, et al. An SU(6) Mott insulator of an atomic Fermi gas realized by large-spin Pomeranchuk cooling. Nat Phys 2012;8:825.
[33] Taie S, Ozawa H, Ichinose T, et al. Coherent driving and freezing of bosonic matter wave in an optical Lieb lattice. Sci Adv 2015;1:1500854.
[34] Scazza F, Hofrichter C, Hofer M, et al. Observation of two-orbital spin-exchange interactions with ultracold SU(N)-symmetric fermions. Nat Phys 2014;10:779.
[35] Cappellini G, Mancini M, Pagano G, et al. Direct observation of coherent interorbital spin-exchange dynamics. Phys Rev Lett 2014;113:120402.
[36] Zhang X, Bishof M, Bromley SL, et al. Spectroscopic observation of SU(N)-symmetric interactions in Sr orbital magnetism. Science 2014;345:1467–73.
[37] Pagano G, Mancini M, Cappellini G, et al. A one-dimensional liquid of fermions with tunable spin. Nat Phys 2014;10:198.
[38] Scazza F, Hofrichter C, Höfer M, et al. Corrigendum: observation of two-orbital spin-exchange interactions with ultracold SU(N)-symmetric fermions. Nat Phys 2015;11:514.
[39] DeSalvo BJ, Yan M, Mickelson PG, et al. Degenerate fermi gas of ^{87}Sr. Phys Rev Lett 2010;105:030402.
[40] Pagano G, Mancini M, Cappellini G, et al. A one-dimensional liquid of fermions with tunable spin. Nat Phys 2014;10:198.
[41] Taie S, Takasu Y, Sugawa S, et al. Realization of a SU(2) × SU(6) system of fermions in a cold atomic gas. Phys Rev Lett 2010;105:190401.
[42] Hofrichter C, Riegger L, Scazza F, et al. Direct probing of the Mott crossover in the SU(N) fermi-Hubbard model. Phys Rev X 2016;6:021030.
[43] DeSalvo BJ, Yan M, Mickelson PG, et al. Degenerate fermi gas of ^{87}Sr. Phys Rev Lett 2010;105:030402.
[44] Maksymenko M, Honecker A, Moessner R, et al. Flat-band ferromagnetism as a Pauli-correlated percolation problem. Phys Rev Lett 2012;109:096404.
[45] Schulenburg J, Honecker A, Schnack J, et al. Macroscopic magnetization jumps due to independent magnons in frustrated quantum spin lattices. Phys Rev Lett 2002;88:167207.
[46] Zhitomirsky ME, Tsunetsugu H. Exact low-temperature behavior of a kagomé antiferromagnet at high fields. Phys Rev B 2004;70:100403.
[47] Derzhko O, Richter J, Honecker A, et al. Universal properties of highly frustrated quantum magnets in strong magnetic fields. J Low Temp Phys 2007;33:745–56.
[48] Derzhko O, Honecker A, Richter J. Low-temperature thermodynamics for a flat-band ferromagnet: Rigorous versus numerical results. Phys Rev B 2007;76:220402.
[49] Stauffer D. Scaling theory of percolation clusters. Phys Rep 1979;54:1–74.
[50] Isichenko MB. Percolation, statistical topography, and transport in random media. Rev Mod Phys 1992;64:961–1043.
[51] Howard G. Lie algebras in particle physics, from isospin to unified theories. 2nd ed. Westview Press; 1999.
[52] Katsura H, Tanaka A. Nagaoka states in the SU(N) Hubbard model. Phys Rev A 2013;87:013617.
[53] Ma ZQ. Group theory for physicists. World Scientific; 2007.
[54] Derzhko O, Richter J, Honecker A, et al. Low-temperature properties of the Hubbard model on highly frustrated one-dimensional lattices. Phys Rev B 2010;81:014421.
[55] Lieb E, Mattis D. Theory of ferromagnetism and the ordering of electronic energy levels. Phys Rev 1962;125:164–72.
[56] Nie WX, Katsura H, Oshikawa M. Ground-state energies of spinless free fermions and hard-core bosons. Phys Rev Lett 2013;111:100402.
[57] Nie WX, Katsura H, Oshikawa M. Particle statistics, frustration, and ground-state energy. Phys Rev B 2018;97:125153.
[58] Derrida B, Vannimenus J. Transfer-matrix approach to percolation and phenomenological renormalization. J Phys Lett 1980;41:473.

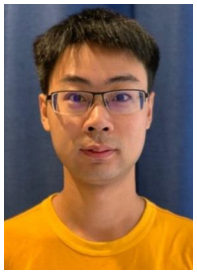

Ruijin Liu received his B.S. degree at Renmin University of China in 2015 and is now a Ph.D. candidate at Renmin University of China under the supervision of Prof. Wei Zhang. His research focuses on strongly correlated fermionic systems with cold atoms.

Wenxing Nie is an associate research professor in College of Physics at Sichuan University. She works theoretically on the fundamental problems of strongly correlated electrons system in condensed matter physics, including SU(N) ferromagnetism, chiral superfluids, quantum spin liquids, and topological materials.

Wei Zhang is a Professor of Renmin University of China. He recently focuses on quantum simulation and computation in artificial quantum systems, including cold atomic gases, optical microcavities, and trapped ions.